

Structure and magnetic properties of $\text{Fe}_x\text{Ni}_{100-x}$ ($25 < x < 100$) and FeCo alloys: Implications for planetary crustal mineralogy. Cécile Cournède¹, Joshua M. Feinberg¹, Catherine L. Johnson^{2,3}, Richard D. James⁴. ¹ Institute for Rock Magnetism, University of Minnesota, Minneapolis, MN, USA (ccournede@umn.edu), ² Department of Earth, Ocean and Atmospheric Sciences, University of British Columbia, Vancouver, BC, V6T 1Z4, Canada, ³ Planetary Science Institute, Tucson, AZ 85719, USA, ⁴ Aerospace Engineering and Mechanics, University of Minnesota, Minneapolis, MN, USA.

Introduction: MESSENGER magnetic field observations revealed the presence of lithospheric magnetizations on Mercury consistent with a combination of induced magnetizations from the present-day core dynamo field and remanent magnetizations recorded early in the planet's history [1, 2]. Mercury's crustal mineralogy likely contains iron-bearing minerals [1, 3-4]. The strongly reducing conditions and elevated temperatures in Mercury's crust and mantle mean that Fe-alloys are the most plausible class of minerals responsible for the majority of Mercury's lithospheric magnetization [5, 6]. Very little information is available regarding the fundamental magnetic properties of Fe-alloys with compositions that are relevant to Mercury (Fe, Ni, and Co alloys). Here we investigate the magnetic properties of metallic alloys covering a wide range of compositions.

Our new Fe-alloy dataset will assist accurate interpretation of the lithospheric magnetic field data from the MESSENGER mission. Moreover beyond Mercury, the results of this study will improve our ability to characterize and interpret the magnetism of a wide array of meteorites.

Samples and methods:

Samples. Iron and nickel wires (2 mm) and Cobalt pellets of 99.995% purity were purchased (Alfa Aesar), cut and mixed in different proportions. Eleven metallic alloys were synthesized under an argon atmosphere with a Thermal Analyst arc melting system in the Department of Aerospace Engineering and Mechanics (UMN). The composition of the alloys are Fe_{100} , $\text{Fe}_{90}\text{Ni}_{10}$, $\text{Fe}_{75}\text{Ni}_{25}$, $\text{Fe}_{60}\text{Ni}_{40}$, $\text{Fe}_{50}\text{Ni}_{50}$, $\text{Fe}_{33}\text{Ni}_{67}$, $\text{Fe}_{30}\text{Ni}_{70}$, $\text{Fe}_{25}\text{Ni}_{75}$, as well as FeCo. Alloys were melted twice to ensure thorough homogenization and masses were checked after each melting step to monitor material lost or gained (e.g., via contamination). Initial compositions of the ~1 cm diameter buttons were obtained using an handheld X-Ray Fluorescence Spectrometer. Impurities were low (<3%) and actual compositions were within 10% of those targeted.

Magnetic investigation. Due to the strong magnetic signal arising from these alloys, smaller subsamples were prepared to enable measurements within the dynamic range of our instrumentation. Three small cylindrical subsamples were obtained (1.5 mm high and 2 mm in diameter) from each button using electrical dis-

charge machining (EDM). All magnetic measurements were collected at the Institute for Rock Magnetism (UMN). Low field susceptibility and its anisotropy were measured using an Agico MFK1 apparatus operating at 976 Hz and 200 Am^{-1} . Frequency and field dependence of susceptibility were evaluated with the MAGNON VFSM.

Hysteresis properties, IRM acquisition and First – order reversal curves (FORCs), were investigated at room temperature using a Princeton Micromag Vibrating Sample Magnetometer (VSM). The saturation remanent magnetization (M_{RS}), saturation magnetization (M_{S}) and the coercive force (B_{C}) were extracted for each sample after a 90% automatic correction of the hysteresis loop. The remanent coercive force (B_{CR}) was determined by back field experiments performed with the VSM. FORCs were processed using the FORCinel Program [7]. Low temperature (10 to 300 K) experiments were carried out using a Quantum Design Magnetic Properties Measurements System (MPMS).

Remanence measurements were performed with a 2G SQUID magnetometer (model 755R, noise level 10^{-11} Am^2) with an attached alternating field (AF) 3-axis demagnetization system. Anhyseretic remanent magnetization (ARM) was imparted using an off-line D-2000 DTech system. The rates of acquisition and decay of viscous magnetization (VRM) of the samples were estimated experimentally.

Composition and Crystallographic analysis. Polished sections were prepared for each alloy. More precise compositional measurements will be made using an electron microprobe analyzer (EMPA). Microstructures within the alloys were observed via optical microscope and SEM, and electron backscatter diffraction is planned to assess the orientation relationships and grain sizes of the microstructures within each alloy. Elemental maps will also be collected using an energy dispersive spectrometry system to characterize compositional differentiation within the alloys.

Preliminary results: An average magnetic susceptibility of $(2.00 \pm 0.06) \times 10^{-4} \text{ m}^3 \cdot \text{kg}^{-1}$ was obtained on the ten FeNi-based alloys and a value of $1.98 \times 10^{-4} \text{ m}^3 \cdot \text{kg}^{-1}$ was obtained for FeCo. Jelinek parameters for anisotropy of magnetic susceptibility [8] indicate an oblate shape for all the synthesized alloys with a mean anisotropy degree, P and shape parameter T of 1.16 and 0.5

respectively. No field or frequency dependence was observed for the alloys. Anhysteretic remanent magnetization and viscous magnetization measurements are challenging on alloys, because these magnetizations are affected by eddy currents in the former case, and by static electricity generation in automated magnetometer sample trays in the latter case. Hysteresis loops and FORC diagrams display multidomain-like behavior (Figure 1), which correlates with optical observations that show grain size $\geq \sim 50 \mu\text{m}$ (Figure 2). 3-axis alternating field demagnetization of saturation isothermal remanent magnetizations yielded low median destructive field values of $\sim 11 \text{ mT}$. In instances where the alloy composition matched those of rare earlier studies, the measured M_s values were in agreement [9, 10].

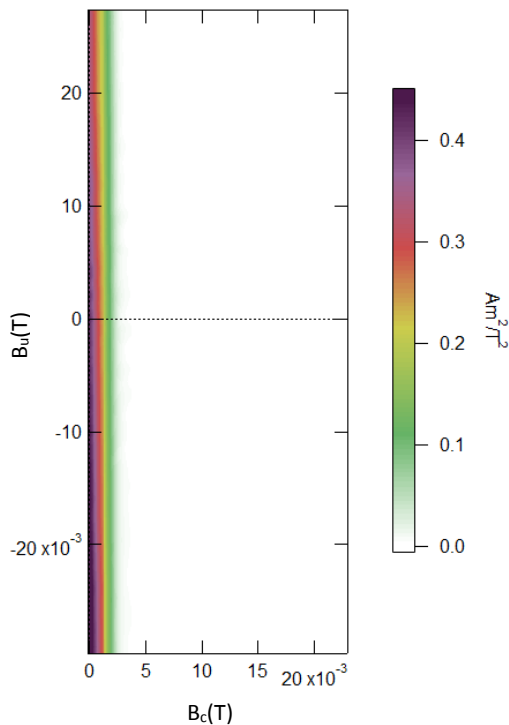


Figure 1: FORC obtained for sample $\text{Fe}_{30}\text{Ni}_{70}$.

Discussion and future work: The magnetic remanence properties of FeNi alloys are dependent on the material's thermal history and on the amount of nickel in the alloy [11]. All of the alloys in this study were prepared under identical synthesis conditions, allowing us to focus on the effects of changing Ni contents. We recognize that the microstructures observed in this study are characteristic of rapidly cooled systems and may not apply to slowly cooled rocks within the crusts of planets or larger asteroids. Our goal was not to reproduce textures observed in slowly-cooled planetary bodies. However, the aim of this study is to provide

constraints on the fundamental magnetic properties of alloys that have received little attention in earlier studies.

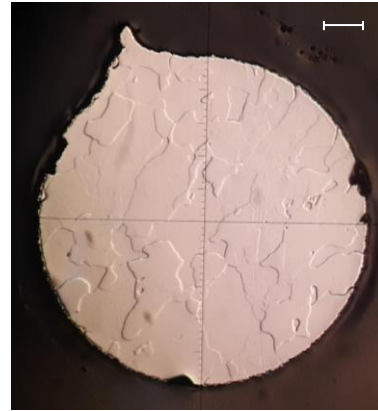


Figure 2: Reflected light optical image of the FeCo polished section. Differential relief indicates the presence of at least two distinct phases. Scale bar is $250 \mu\text{m}$.

Experiments are planned to measure thermal remanence acquisition and Curie temperatures using a Physical Properties Measurement System (PPMS) for each alloy. Information on microstructures will be important for understanding the observed magnetic behavior, including coercivity, induced magnetization, VRM acquisition and much more.

References: [1] Johnson C. L. et al. (2015) *Science*, 348, 892-895. [2] Johnson C. L. et al. (2018) *LPS, XLIX*, Abstract #1505. [3] Strauss B. et al. (2016) *Journal of Geophysical Research, Planets*, 121, 2225-2238. [4] Nittler L. R. et al. (2011) *Science*, 333, 1847-1850. [5] Vander Kaaden K. E. and McCubbin F. M. (2015) *JGR-Planets*, 120, 195-209. [6] Vander Kaaden K. E. et al. (2017) *Icarus*, 285, 155-168. [7] Harrison R. J. and Feinberg J. M. (2008) *Geochemistry Geophysics Geosystems*, 9, Q05016. [8] Jelinek V. (1981) *Tectonophysics*, 79, 63-67. [9] Wack M. et al. (2018) *Magnetic Fields in the Solar System*, 383-406. [10] Sanchez-De Jesus F. et al. (2016) *Journal of Metallurgy*, 2016. [11] Wasilewski P. (1981) *The Moon*, 9, 335-354.